Extended Abstracts of the 2014 International Conference on Solid State Devices and Materials, Tsukuba, 2014, pp316-317

Effects of interface electric field on the magnetoresistance for nonlocal setup

Tetsufumi Tanamoto*, Mizue Ishikawa, Tomoaki Inokuchi, Hideyuki Sugiyama, and Yoshiaki Saito[1]

[1]*Advanced LSI Technology Laboratory Toshiba R and D Center, Kawasaki 212-8582, Japan.*
**Phone:+81-44-549-2315, E-mail:tetsufumi.tanamoto@toshiba.co.jp*

Abstract

The effect of the interface electric field on the non-local measurement setup is discussed both theoretically and experimentally. We found that the interface electric fields increase the spin polarization when the depletion region grows.

1. Introduction

One of the important issues of spintronics[1-3] is the spin injection and detection between ferromagnet and semiconductor, which is sensitive to the interface properties. In the last paper [4], we showed that, for the local measurement setup, the electric field at the interface greatly changes the magnetoresistance (MR) ratio depending on the direction and the strength of the electric field. In this paper, we discuss the effect of the interface electric field for the nonlocal setup depicted in Fig.1. We found that the interface electric field affects the MR ratio in a different form from those of the local measurement setup.

2. Formulation

We introduce a quantum effect as the density-gradient (DG) term [5] to the spin dependent chemical potentials. The DG term is expressed by $b\nabla^2\sqrt{n_s}/\sqrt{n_s}$ with $b=\hbar^2/(2mer_q)$ and the density of carrier n_s ($s=\uparrow,\downarrow$, $\nabla=\partial/\partial z$). The parameter r_q changes depending on physical environment (we take $r_q=2$ here) [5]. Similar differential equations as those of the standard diffusion theory are held by replacing the chemical potential by that with the DG term, $\mu^*_\pm$, such as, $\frac{e}{\sigma_\pm}\frac{\partial J_\pm}{\partial z}=\pm\frac{\mu^*_+-\mu^*_-}{l^2_{sf}}$ and $\frac{\partial^2(\mu^*_+-\mu^*_-)}{\partial z^2}=\frac{(\mu^*_+-\mu^*_-)}{l^2_{sf}}$ (l_{sf} is the spin diffusion length l^N or l^F).

The generalized drift-diffusion equations are solved depending on the geometry of the nonlocal measurement setup of Fig.1 by extending Ref.[3]. The chemical potentials are described as

$$\mu^{(\mathrm{I})}_\pm = A-\frac{J_Le}{\sigma_F}x\pm\frac{2C}{\sigma_F(1\pm\beta)}e^{-\frac{x}{\lambda_F}}-\psi_{Ab\pm}(x), \quad (1)$$

$$\mu^{(\mathrm{II})}_\pm = -\frac{J_Le}{\sigma_N}x\pm\left[\frac{2E}{\sigma_N}e^{-\frac{x}{\lambda_N}}+\frac{2F}{\sigma_N}e^{\frac{x}{\lambda_N}}\right]-\psi_{Eb\pm}(x), \quad (2)$$

$$\mu^{(\mathrm{III})}_\pm = \pm\frac{2G''}{\sigma_N}e^{-\frac{x}{\lambda_N}}-\psi_{Gb\pm}(x), \quad (3)$$

$$\mu^{(\mathrm{IV})}_\pm = \frac{J_Me}{\sigma_N}x\pm\frac{2G}{\sigma_N}e^{-\frac{x}{\lambda_N}}-\psi_{Kb\pm}(x), \quad (4)$$

$$\mu^{(\mathrm{V})}_\pm = \pm\left[\frac{2H}{\sigma_N}e-\frac{x}{\lambda_N}+\frac{2K}{\sigma_N}e^{\frac{x}{\lambda_N}}\right]-\psi_{Hb\pm}(x), \quad (5)$$

$$\mu^{(\mathrm{VI})}_\pm = B\pm\frac{2D}{\sigma_F(1\pm\beta)}e^{-\frac{x}{\lambda_F}}-\psi_{Bb\pm}(x), \quad (6)$$

$$\mu^{(\mathrm{VII})}_\pm = \pm\left[\frac{2G_1}{\sigma_N}e^{-\frac{x}{\lambda_N}}+\frac{2G_2}{\sigma_N}e^{\frac{x}{\lambda_N}}\right]-\psi_{G_1b\pm}(x), \quad (7)$$

where β is a spin polarization. A-G,G'',G_1 and G_2 are unknown coefficients to be determined by the boundary conditions and the current conservation conditions. $\psi^F_{b\alpha\pm}$ and $J^F_{b\alpha\pm}$ are the quantum effects given by $\psi^F_{b\alpha\pm}=\left(2b/\sqrt{n^F_{\alpha\pm}}\right)\nabla^2\sqrt{n^F_{\alpha\pm}}$, $\psi^N_{b\pm}=\left(2b/\sqrt{n^N_{\pm}}\right)\nabla^2\sqrt{n^N_{\pm}}$, $J^F_{b\alpha\pm}=2(\sigma_\pm/e)\nabla\psi_{b\alpha\pm}$, and $J^F_{b\pm}=2(\sigma_N/e)\nabla\psi_{b\pm}$. We write $\rho_\pm=2[1\pm\beta]\rho_F$ and ρ_N for the resistivity of the ferromagnet F and the semiconductor N. For the antiparallel case, we have $\mu^{(\mathrm{VI})}_\pm=B\mp\frac{2D}{\sigma_F(1\mp\beta)}e^{-\frac{x}{\lambda_F}}-\psi_{Bb\mp}(x)$. Current is obtained from $J_s=\frac{\sigma_s}{e}\frac{\partial\mu^*_s}{\partial x}$ with conductance $\sigma_\pm=\frac{1}{2\rho_F(1\mp\beta)}=\frac{(1\pm\beta)}{2}\sigma_F$. Then the currents are expressed by

$$J^{(\mathrm{I})}_\pm = -\frac{1\pm\beta}{2}J_L\mp\frac{C}{e\lambda_F}e^{-\frac{x}{\lambda_F}}-J_{Ab\pm}(x), \quad (8)$$

$$J^{(\mathrm{II})}_\pm = -\frac{1}{2}J_L\mp\left[\frac{E}{e\lambda_N}e^{-\frac{x}{\lambda_N}}-\frac{F}{e\lambda_N}e^{\frac{x}{\lambda_N}}\right]-J_{Eb\pm}(x), \quad (9)$$

$$J^{(\mathrm{III})}_\pm = \mp\frac{G''}{e\lambda_N}e^{-\frac{x}{\lambda_N}}-J_{G''b\pm}(x), \quad (10)$$

$$J^{(\mathrm{IV})}_\pm = \frac{J_M}{2}\mp\frac{G}{e\lambda_N}e^{-\frac{x}{\lambda_N}}-J_{Kb\pm}(x), \quad (11)$$

$$J^{(\mathrm{V})}_\pm = \mp\left[\frac{H}{e\lambda_N}e^{-\frac{x}{\lambda_N}}-\frac{K}{e\lambda_N}e^{\frac{x}{\lambda_N}}\right]-J_{Hb\pm}(x), \quad (12)$$

$$J^{(\mathrm{VI})}_\pm = \mp\frac{D}{e\lambda_F}e^{-\frac{x}{\lambda_F}}-J_{Bb\pm}(x), \quad (13)$$

$$J^{(\mathrm{VII})}_\pm = \mp\left[\frac{G_1}{e\lambda_N}e^{-\frac{x}{\lambda_N}}-\frac{G_2}{e\lambda_N}e^{\frac{x}{\lambda_N}}\right]-J_{G_1b\pm}(x), \quad (14)$$

The geographical difference from Ref.[3] is that there is a region (VII) in the present case. The same boundary conditions on chemical potential and current at an interface $z=z_\alpha$ ($\alpha=L,R$) are given by $\mu_\pm(z^+_\alpha)-\mu_\pm(z^-_\alpha)=r_\pm J_\pm(z_\alpha)$ and $J_\pm(z^+_\alpha)=J_\pm(z^-_\alpha)$. We also define $r^\alpha_\pm=2r_b[1\pm\gamma^\alpha]$, $r^\alpha_p=[r^\alpha_++r^\alpha_-]/4=r_b$, $r^\alpha_m=[r^\alpha_--r^\alpha_+]/4=r_b\gamma^\alpha$, $r_F=\rho_Fl^F$, $r_N=\rho_Nl^N$. The important quantities here are $r_F\equiv\rho_Fl^F$ and $r_N\equiv\rho_Nl^N$. After a long straightforward calculation, the spin-dependent resistance ΔR is obtained by

$$\Delta RS=\frac{4c_R}{\Theta_1[J_L+\sigma_Fu_A](1-\beta^2)}\Big\{r_N(1-\beta^2)c_L(J_L+\sigma_Fu_A) -\sigma_Fu_Bc_R\Big\{B^L_p\left(\nu_3b_5+\frac{\nu_4}{b_5}\right)b_2+B^L_m\left(\nu_1b_5+\frac{\nu_2}{b_5}\right)/b_2\Big\}\Big\}, \quad (15)$$

The spin polarization $P=\frac{J_+-J_-}{J_++J_-}$ is expressed by

$$P=\frac{1}{\Theta_1(J_L+\sigma_Fu_A)}\frac{S_R}{S_L}\Big\{-4r_N(1-\beta^2)\sigma_Fu_Bc_R +c_L(J_L+\sigma_Fu_A)\Big\{B^R_p\left[1+\frac{2S_N}{S_R}\right]+B^R_m\left[1-\frac{2S_N}{S_R}\right]\Big\}u\Big\}. \quad (16)$$

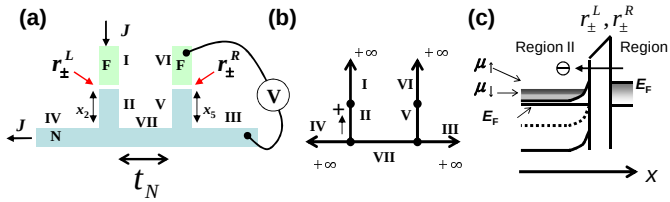

FIG. 1: (a) Nonlocal setups. F (Region I and VI) shows a magnetic electrode. Other parts consist of semiconductor(N). Here, we consider the effects of the interface electric field E_L^N at the I-II and E_R^N at the V-VI interface. (b) Diagram of the chemical potential solutions. The nodes represent the origins of the coordinate axes in the seven regions, and the arrows indicate the positive x directions. (c) Band structure at the interface between the regions F and N.

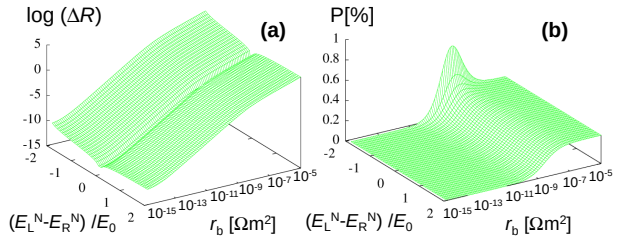

FIG. 2: (a) ΔR and (b) P as functions of the tunneling resistance r_b and the interface electric field. $E_0 \equiv J/\sigma_F$. $\gamma_L = \gamma_R = 0.5$ $l_N = 1$ μm, $r_N = 4.0\times10^{-9}\Omega$ m^2, $l_F = 5$ nm, $\beta = 0.46$, $r_F = 4.5\times10^{-15}$ Ω m^2.

where $u = e^{t_N/\lambda_N}$, $\nu_1 = \{(1-2w_M)(2+w_R)u - w_R/u\}/4$, $\nu_2 = \{(1-2w_M)(2-w_R)u + w_R/u\}/4$, $\nu_3 = \{(1+2w_M)(2+w_R)u - w_R/u\}/4$, $\nu_4 = \{(1+2w_M)(2-w_R)u + w_R/u\}/4$. Moreover, $B_p^\alpha = [r_N + r_p^\alpha](1-\beta^2) + r_F$, $B_m^\alpha = [r_N - r_p^\alpha](1-\beta^2) - r_F$, $c_\alpha = r_F\beta + r_m^\alpha(1-\beta^2)$ for $\alpha = L, R$, and $\Theta_1 = B_m^R/b_5(\nu_2 B_m^L/b_2 + \nu_4 B_p^L b_2) - B_p^R b_5(\nu_1 B_m^L/b_2 + \nu_3 B_p^L b_2)$. $u_A = E_L^N/r_a$ and $u_B = E_R^N/r_a$ are the interface electric field for the two interfaces. These formula are reduced to those of Ref.[3] when there is no electric field. We can see that E_L^N and E_R^N differently affect P and ΔR. This analytical form shows that, as the interface electric fields E_L^N and E_R^N increase, P decreases. This is the opposite result of the local measurement of Ref. [4].

Fig. 2 shows the result of numerical calculations as a function of the electric field $(E_L^N - E_R^N)$ and the tunneling resistance r_b for ΔR and P. We can see an increase of P at the left side where the electric field is negative. These are the results of the additional terms in Eq.(15) and Eq.(16).

4. Experiments

We fabricated four-terminal devices for Hanle-effect measurements, as shown in Fig. 3(a) for two types of different area configurations: [A] $S_L = 50\mu$m^2, $S_R = 200\mu$m^2 and $t_N = 2050$ nm, [B] $S_L = 40\mu$m^2, $S_R = 50\mu$m^2 and $t_N = 1250$ nm. The CoFe/MgO is patterned on a phosphorus-doped ($\sim 2\times10^{19}$ cm^{-3}) (100) textured Si of an insulator (SOI) substrate[4,6]. Fig. 3(b)(c) show

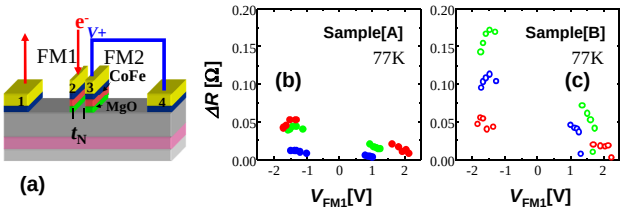

FIG. 3: (a) Four-terminal devices used in the experiment. (b)(c) Measured ΔR as a function of the junction bias for the two samples with different MgO thickness t. The red, green and blue dots show data for $t = 1.5, 1.6, 1.8$nm for the sample [A] and $t = 1.3, 1.5, 1.8$nm for [B].

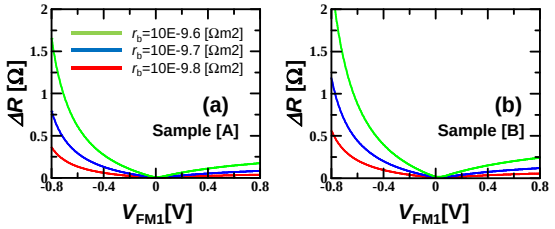

FIG. 4: Calculated ΔRs as a function of the interface electric field for (a) sample [A] and (b) sample [B]. As suggested in Fig.2, ΔR for negative interface electric field is larger than that of the positive side. These are the results of the interface electric field (See the 2nd term of Eq.(15)). $\gamma_L = \gamma_R$.

ΔR for different MgO thickness (t) ($t = 1.5, 1.6, 1.8$nm for the sample [A] and $t = 1.3, 1.5, 1.8$nm for [B]). We can see that ΔR of the sample [B] is more sensitive to the MgO thickness than that of the sample [A]. This is because t_N of the former is shorter than the latter.

5. Comparison with experiments

Fig. 4 shows calculated ΔR as a function of the interface electric field for the two samples. The change of the MgO thickness of Fig 4 can be taken into account in the calculation by changing the interface resistance r_b. Because of the additional terms in Eq.(15), ΔR for negative interface electric field is larger than that of the positive side. Physically, the enhancement comes from the extension of the depletion region.

6. Conclusions

We have investigated the effect of the interface electric field on the non-local measurement setup both theoretically and experimentally. It is found that the interface electric fields affect the spin polarization and resistance change such that the spin polarization is enhanced when the depletion regions grows.

References

[1]S. Sugahara *et al.*, Appl. Phys. Lett. 84 2307 (2004).
[2]T. Inokuchi *et al.*, VLSI Symp 2010, p119.
[3]F. J. Jedema *et al.*, Phys. Rev. B **67** 085319 (2003).
[4]T. Tanamoto *et al.*, J.Appl,Phys.115, 163907 (2014).
[5]M.G. Ancona *et al.*, Phys. Rev. B **35**, 7959 (1987).
[6]M. Ishikawa *et al.*, J. Appl. Phys **114** 243904 (2013).